Processing of Poly(2,6-dimethyl-1,4-phenylene ether) with Epoxy Resin. 2. Gelation Mechanism

Yoshiyuki Ishii† and Anthony J. Ryan*

Department of Chemistry, The University of Sheffield, Brookhill, Sheffield, S3 7HF, UK

Received May 28, 1999; Revised Manuscript Received November 1, 1999

ABSTRACT: Poly(2,6-dimethyl-1,4-phenylene ether) (PPE), having a low dielectric constant and high T_g, is traditionally difficult to process without the use of solvents. To enable processing, PPE is dissolved into epoxy resin, and the gelation mechanism is studied chemorheologically. The gelation was followed by rheometry using multifrequency methods. The gel point of neat epoxy was at a conversion of epoxy ≃0.60, which agreed with the prediction of Flory−Stockmayer gelation theory. However, the gel point of the PPE/epoxy mixture depended on the curing temperature and occurred at a lower extent of reaction than that of the neat epoxy. The gelation of PPE/epoxy blends is the vitrification of a PPE-rich matrix following phase separation and not chemical gelation. Prediction of the phase diagram during reaction can be achieved using Flory−Huggins theory for phase separation and recursive theory for gelation.

Introduction

Understanding the processing of thermosets is a difficult task, because of the insoluble, cross-linked nature of these polymers. To overcome the complexities of thermoset processing, "chemorheological" techniques are powerful tools. In this context "chemorheology" is defined as the study of viscoelastic behavior of a reacting system[1] and encompasses knowledge of the variation in viscosity due to chemical reaction and processing conditions and characterization of the growth of the infinite molecular network and the immobilized glassy state. The interaction between these two phenomena is obvious, because the rate of rheological change in either the liquid or solid and the development of the optimum glass transition temperature cannot be separated from the polymerization chemistry. Particularly in the case of thermoplastic/thermoset blends, phase separation has to be considered in rheological and kinetic terms because the Flory−Huggins mixing equation is significantly sensitive to the molecular weight.[2,3] Consideration of phase diagrams during polymerization is necessary to explore the physical and chemical processes taking place in thermoplastic/thermoset alloys.

The type of phase diagram that needs to be considered in reaction-induced phase separation (RIPS) depends on the mechanism of polymerization and the T_g−composition curve. In free radical polymerizations, there are only two components present in any appreciable concentration, monomer and high molecular mass polymer; the growing chains have a small instantaneous concentration. Thus, a ternary phase diagram is appropriate for understanding RIPS. In step polymerizations, the molecular weight distribution evolves gradually, and there is a continuous (most probable) distribution of molar mass and the system can be considered as a pseudobinary.

Goossens et al.[4] studied the structure development during reaction-induced phase separation in polyethylene/styrene system. Liquid−liquid phase separation and crystallization of polyethylene occurred simultaneously during styrene polymerization. Structure development in the ternary mixture was investigated by time-resolved small-angle X-ray scattering (SAXS) and wide-angle X-ray scattering (WAXS). Ternary phase diagram are required to understand structure development in PE/polystyrene/styrene because the mixture contains high molar mass polystyrene and styrene monomer throughout. Liquid−liquid phase separation was followed by a liquid−solid transition in the polyethylene-rich domains when the isothermal polymerization temperature was below the crystallization temperature of polyethylene. In contrast, binary phase diagrams are appropriate for predicting step growth reactions, such as polyurethanes, polyureas, and epoxy resins, because the gradual buildup in molecular weight in step polymerizations allows them to be considered a single phase. However, the glass transition−composition curve (Fox equation) in the phase diagram must be considered. Inoue[5] studied the polyether sulfone/epoxy system. This binary mixture has a lower critical solution temperature (LCST)-type phase diagram. Once curing starts, the LCST is expected to decrease, and the two-phase regime would prevail in the phase diagram as the molecular weight of epoxy increases with curing. The T_g of the mixture, which is estimated by the Fox equation, would rise as the molecular weight is increased. The intersection between the coexistence curve and the Fox equation is called Berghman's point[6] and is significant for considering phase diagrams of polymers because once the composition reaches that point, no further separation is possible.

There have been only a few theoretical attempts to explain the phase diagram of reaction-induced phase separation due to the complex interaction between phase separation and cross-linking. Clarke[7] developed a novel prediction of a phase diagram for thermoplastic/thermoset blends. This treatment was based on the miscibility of linear polymers with branched or star polymers. To obtain a series of snapshots of the phase diagram during polymerization, it is necessary to know the molecular weight of the linear component, the molecular weight distribution of the branched polymer, and χ parameter for the system. Using small-angle neutron scattering and GPC, these parameters were

† Current address: Fabrication Technology Laboratory, Asahi Chemical Industry, Co., ltd. Yakoh, Kawasaki, 210-0863, Japan.
* To whom all correspondence should be addressed.

10.1021/ma990838a CCC: $19.00
Published on Web 12/16/1999

obtained, and phase diagrams under isothermal cure were successively predicted.[8]

There is a plethora of literature concerning blends of thermoplastics and thermosets, and these are often termed semiinterpenetrating networks or semi-IPN; see for example the review by Mishra and Sperling.[9a] The aspects of interest here, the interaction between polymerization and the phase behavior, have been reported in the context of semi-IPN by Mishra et al. [9b]

In the preceding paper,[10] reaction-induced phase separation of PPE/epoxy blends was investigated using time-resolved light scattering equipment equipped with an optical DSC. Laser light scattering measurements characterize the subsequent spinodal decomposition process. Cahn−Hilliard linear theory yields initial correlation lengths and effective interdiffusion coefficients and accounts for the early stage of the spinodal decomposition. The morphology and mechanical properties of the cured blend were investigated by SEM, TEM, and DMTA. This paper focuses on the chemorheological study of PPE/epoxy mixtures. Reaction kinetics were followed by isothermal DSC. Gelation was followed using dynamic mechanical measurement, and the gel point was determined rheologically. The obtained results are interpreted in terms of a pseudobinary phase diagram.

Experimental Section

PPE, epoxy resin (AER260), and diethyltoluenediamine (DETDA) were used as received and mixed in a Brabender plastograph kneader. Details of the materials and blending were described in the preceding paper.[10]

Differential scanning calorimetry (DSC) was used for kinetic studies of the network formation and T_g determination of the blend. A Dupont 2000 thermal analyzer equipped with a DSC 990 cell was operated under a nitrogen atmosphere; samples of ~10 mg were encapsulated in aluminum pans. For dynamic DSC, the pan was cooled to −100 °C on the DSC head and then heated at 10 °C/min. Measurements of heat flow and against time and temperature were made, with respect to a reference. For isothermal measurements, an aluminum sample pan was inserted into the DSC cell at the required temperature, and equilibrium was established in less than 1 min. The rate of enthalpy evolution was followed with time. The isothermal heat flow curve was obtained to subtract the baseline signal, assuming that the difference in heat capacity before and after reaction is negligible.

In rheological experiments, multifrequency oscillatory-shear experiments were performed in a Rheometrics RMS 800 rheometer using the multifrequency experimental method. The gel time of the reaction was determined using the tan δ congruency for all the frequencies tested. Experimentally, the parallel plates were preheated to the operating temperature before a zero gap was set. The upper plate was then raised, and the mixture was put on the lower plate. The measurement was started as soon as the temperature reached the operating temperature. Frequencies used for the measurement were 1, 10, 20, 40, 60, 80, and 100 Hz. Applied strains ranged from 1% to 5% and were in the linear viscoelastic regime.

Results and Discussion

Reaction Kinetics. (a) Reaction Kinetics for Epoxy/Amine. The curing of an epoxy with a primary amine involves two principal reactions, i.e., the reaction between the primary amine hydrogen and epoxy to form a secondary amine and the reaction between the secondary amine hydrogen and epoxy to form a tertiary amine.[11] Both reactions are catalyzed by the hydroxyl groups formed during the reaction. Horie[12] has derived the reaction scheme to describe the overall kinetics of the epoxide reaction with primary amine, taking into account the autocatalytic reaction of the hydroxyl groups generated during the reaction and assuming that some catalyst or impurity is initially present in the system:

$$A_1 + E + (HX)_a \xrightarrow{k_1} A_2 + (HX)_a + (HX)_a \quad (1)$$

$$A_1 + E + (HX)_0 \xrightarrow{k'_1} A_2 + (HX)_0 + (HX)_a \quad (2)$$

$$A_2 + E + (HX)_a \xrightarrow{k_2} A_3 + (HX)_a + (HX)_a \quad (3)$$

$$A_2 + E + (HX)_0 \xrightarrow{k'_2} A_3 + (HX)_0 + (HX)_a \quad (4)$$

where A_1, A_2, and A_3 are primary, secondary, and tertiary amines, respectively. E is the epoxy group, $(HX)_a$ is the pendant hydroxyl groups on the backbone of the reaction products, and $(HX)_0$ is the initial catalyst or impurity. Kamal[13] proposed an empirical equation to describe an autocatalytic reaction. Gillham[14] also derived the reaction rate for an initial stoichiometric mixture of epoxy and amine by assuming equal reactivity of all amine hydrogens. The equation is expressed by an extent of reaction (p) as

$$dp/dt = k(1 - p)^2(p + B) \quad (5)$$

where $k = k_1e_0^2/2$, $B = k'_1c_0/k_1e_0$, and e_0 and c_0 are the initial concentrations of epoxide groups and $(HX)_0$, respectively. Equation 5 is used to analyze the reaction kinetics of the present system by rearranging in the following form:

$$\frac{dp/dt}{(1 - p)^2} = k'p + k''B \quad (6)$$

Dynamic and isothermal DSC have been used to analyze the epoxy−amine kinetics.

The DSC scan from 0 to 350 °C at a heating rate of 10 °C/min for a stoichiometric mixture of the epoxy/DETDA is shown as an inset to Figure 1. A single, moderately broad reaction exotherm is observed with a maximum temperature at 200 °C. Above 300 °C another exotherm is observed due to the thermal degradation of cured epoxy resin. The heat of reaction of the epoxy/DETDA cure was found to be 265 J/g, which is a reasonable value compared to those reported bisphenol A type epoxy resin and aromatic amine compound.[11] Figure 1 shows heat flow vs time curves obtained by isothermal DSC for the epoxy/DETDA system at different temperature. They clearly show the rapid increase in the reaction rate followed by an exponential decrease with time, ending in a flat line. Figure 2 is a plot of $(dp/dt)/(1 - p)^2$ vs extent of reaction p, for various isothermal conditions. The data follow a straight line up to the gel point. The nonzero value of B indicates the presence of an initial, trace catalyst accelerating the reaction in the system. This could be a small amount of hydroxyl groups initially in the diepoxide monomer or

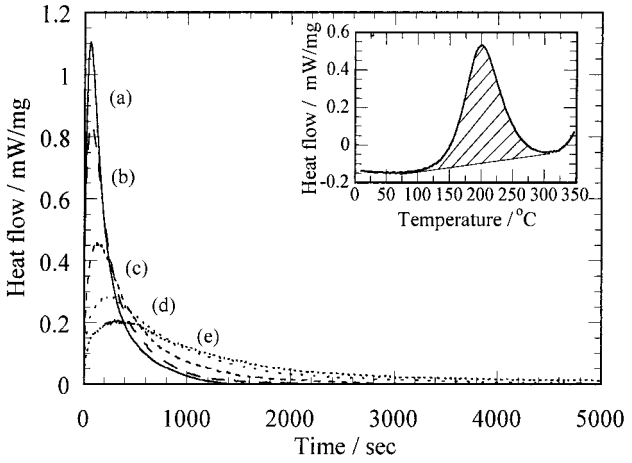

Figure 1. DSC curves of epoxy/DETDA cured isothermally at (a) 200 °C, (b) 195 °C, (c) 175 °C, (d) 160 °C, and (e) 150 °C. The inset is a DSC curve of epoxy/DETDA heating at 10 °C/min.

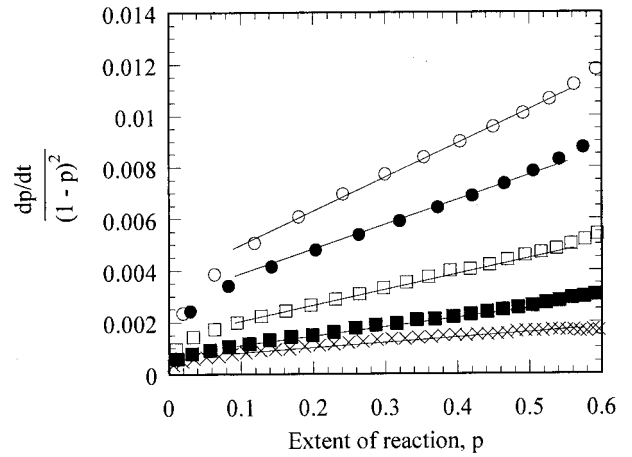

Figure 2. Autocatalytic kinetic expression for the isothermally cured epoxy/DETDA system for (○) 200 °C, (●) 195 °C, (□) 175 °C, (■) 160 °C, and (×) 150 °C.

the end groups of PPE. The autocatalytic reaction model has been used by other investigators to describe the chemical kinetics of a variety of aromatic amine-cured epoxy systems and has been found to be applicable over a wide conversion range. This study also suggests that the autocatalytic model is appropriate for the epoxy/DETDA system.

(b) Reaction Kinetics for PPE/Epoxy/Amine. The dynamic DSC curing of the PPE/epoxy/DETDA system is illustrated in the inset to Figure 3. The influence of PPE on the epoxy−amine curing system is apparent in reducing the reaction rate (exotherm peak maximum shifted from 200 to 215 °C) and change of specific heat (slight discrepancy in baseline). The reduction in reaction rate is due to the high viscosity of the homogeneous mixture and, of course, to the reduction in functional group concentration. The change of specific heat is attributed to the vitrification of PPE. Isothermal DSC curing of a PPE/epoxy/DETDA system containing 30 wt % of PPE is illustrated in Figure 3. The isothermal scan of PPE/epoxy/DETDA also shows the reduced reaction as observed in dynamic DSC. After an induction period, a increased reaction rate was observed (indicated by the arrow). This phenomenon is due to the liquid−liquid phase separation which proceeds to form low-viscosity epoxy−amine droplets in a PPE-rich matrix.[15] As the

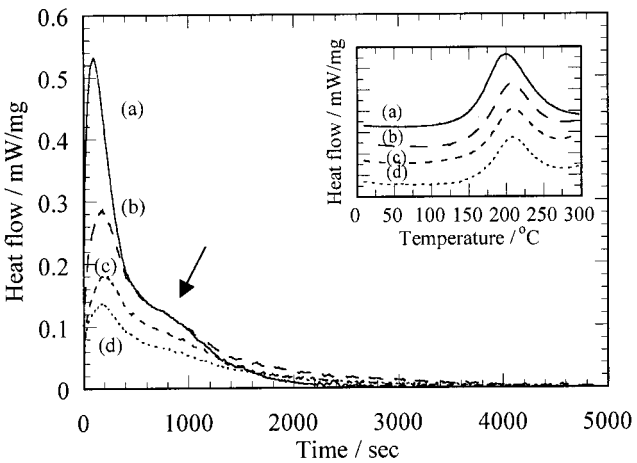

Figure 3. DSC curves of the PPE/epoxy /DETDA cured isothermally at (a) 195 °C, (b) 175 °C, (c) 160 °C, and (d) 150 °C. PPE content is 30 wt %. The inset is DSC curves of PPE/epoxy/DETDA heating at 10 °C/min. PPE content is (a) 0 wt %, (b) 30 wt %, (c) 40 wt %, and (d) 50 wt %. The arrow indicates the recovery of reaction rate.

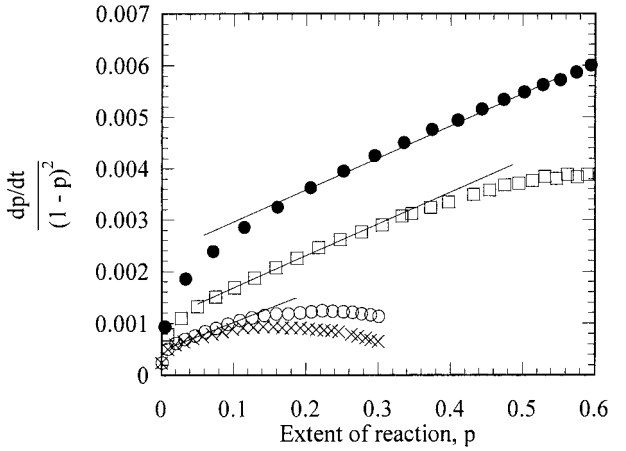

Figure 4. Autocatalytic kinetic expression for the isothermally cured PPE/epoxy/DETDA system for (●) 195 °C, (□) 175 °C, (■) 160 °C, and (×) 150 °C. PPE content is 30 wt %.

PPE content increases, the inflection point becomes difficult to observe. This is due to slow reaction rate and small exotherm of the overall reaction. The effects of heterogeneous structure can be understood by the plot of the kinetic expression as shown in Figure 4. The reaction rate which is proportional to the slope of the curve in the second-order kinetics plot decreases significantly as the reaction proceeds toward the end, which suggests that the reaction may run into a diffusion-limited regime. These results indicate that diffusion effects and the emerging microphase have to be considered at the same time for curing a thermoplastic/thermoset blends.

***T_g* and Molecular Weights as a Function of Conversion in Epoxy/Amine.** Predicting and controlling Berghman's point is particularly important in the case of reactive melt processing. In this section, T_g and molecular weights of epoxy resin are theoretically estimated as a function of chemical conversion. The dependence of the T_g on the extent of reaction is measurable through thermal analysis. The development of the coexistence curve is also predictable as a function of the molecular weight of the epoxy resin. Both curves are used for a prediction of phase diagram of PPE/epoxy in a later section.

Table 1. Expressions Used To Calculate Network Parameters for Stoichiometric Mixtures of Bifunctional Epoxy and Tetrafunctional Amine Network System[a]

network parameter	expression
number-average molecular weight (M_n)	$(M_{epoxy} + {}^1/_2 M_{amine})/({}^3/_2 - 2p)$
weight-average molecular weight (M_w)	$[{}^1/_2(M_{amine})^2(1+p)^2 + M_{epoxy}(1+3p)^2 + 4M_{epoxy}M_{amine}]/[{}^1/_2(M_{amine} + M_{epoxy})(1-3p^2)]$
gel point	0.577
probability of finite chain (P)	$(1/p^2 - {}^3/_4)^{1/2} - {}^1/_2$
sol fraction (w_s)	$(1/p^2 - {}^3/_4)^{1/2} - {}^1/_2)^4$
gel fraction (w_g)	$1 - w_s$
effective cross-link density (4-functional)	$4P(1-P)^3$
effective cross-link density (3-functional)	$(1-P)^4$

[a] M_{epoxy} = molecular weight of epoxy resin; M_{amine} = molecular weight of amine.

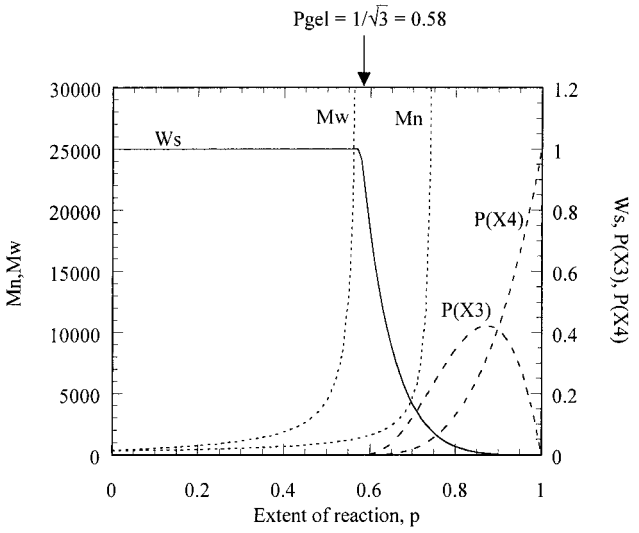

Figure 5. Calculated molecular weights (M_n, M_w) and other properties for the epoxy network formation of this system. W_s is a sol fraction; P(X3) and P(X4) are relative concentrations of the amine cross-linking unit of degree of 3 and 4, respectively. Initial molecular weights for epoxy and amine are 381 and 178, respectively. Flory−Stockmayer's gel point for a stoichiometric mixture of 2-functional epoxy and 4-functional amine (0.58) is indicated in the figure.

A treatment to describe the variation of T_g during curing has been proposed by Wisanrakkit and Gillham[14] and Yang and Macosko[16]. They assumed that in the pregel region the glass transition is a function of molecular weight only. In the postgel region, the system is regarded as a miscible binary mixture of sol and gel fractions. Gillham used bisphenol A type epoxy and aromatic diamine, whereas Macosko used model compounds to determine the parameters in the pregel region and applied them to the novolac epoxy system. In this study, T_g and molecular weight as a function of chemical conversion are calculated in accordance with Gillham's method.

Molecular weight and other parameters can be expressed by the extent of reaction using recursive theory.[17] Table 1 summarizes molecular weight, sol, gel fraction, probability of finite chain, and the cross-link density of a stoichiometric mixture of the bifunctional epoxy and a tetrafunctional amine network system. These expressions are also illustrated in Figure 5 using the molecular weights of the epoxy and amine used in this study.

Prior to gelation ($p < 0.58$), the T_g of the mixture is equal to that of sol. Fox and Loshaek[18] have shown that the T_g of the linear homogeneous polymer can be directly related to the number-average molecular weight.

$$1/T_g = 1/T_{g(\text{linear, infinite})} + K_n/M_n \tag{7}$$

where $T_{g(\text{linear, infinite})}$ is the glass transition temperature of an infinitely long linear polymer, and K_n is a constant. Equation 7 is adopted for calculating the T_g of the sol fraction, despite the sol fraction consisting of both linear and branched molecules. The constant, K_n, will change with the number of chain ends. However, for simplicity, K will be treated as a constant.

The number-average molecular weight for a stoichiometric mixture is

$$M_n = \frac{M_n(0)}{1 - {}^4/_3 p} \tag{8}$$

where $M_n(0)$ is the number-average molecular weight of the initial mixture. Substituting eq 8 into eq 7 yields

$$\frac{1}{T_g} = \frac{1}{T_{g(\text{linear, infinite})}} + \frac{K}{M_n(0)}\left(1 - \frac{4}{3}p\right) \tag{9}$$

$T_{g\ (\text{linear, infinite})}$ can be determined by substituting $p = 0$ into eq 9:

$$\frac{1}{T_{g(\text{linear, infinite})}} = \frac{1}{T_{g(0)}} - \frac{K}{M_n(0)} \tag{10}$$

Thus,

$$\frac{1}{T_g} = \frac{1}{T_{g(0)}} - \frac{4Kp}{M_n(0)} \tag{11}$$

The constant in eq 11 can be determined by fitting $1/T_g$ vs conversion before the gel point. Thus, the relationship between T_g and conversion before gel point can be expressed by eq 11.

After the gel point the system can be considered a mixture of sol and gel. From an empirical rule of mixing the T_g of the binary mixture is given by

$$\frac{1}{T_g} = \frac{w_s}{T_{gs}} + \frac{w_g}{T_{gg}} \tag{12}$$

where w_s and w_g are the weight fractions for the sol and gel fraction, and T_{gs} and T_{gg} are glass transition temperatures of the sol and gel. T_g of the sol fraction is

$$\frac{1}{T_{gs}} = \frac{1}{T_{g(\text{linear, infinite})}} + \frac{K}{M_n(\text{sol})} \tag{13}$$

where M_n(sol) is the number-average molecular weight of the sol fraction, which can be calculated by the recursive method.

T_g of the gel fraction can be evaluated from the Fox and Loshaek equation for a finite polymer chain with cross-links,

$$T_{gg} = T_{g(\text{linear, infinite})} - K/M_n + K_x\rho \qquad (14)$$

where ρ is the cross-link density, and K_x is a constant. The number-average molecular weight of the gel fraction is infinite; therefore, eq 14 can be rewritten to

$$T_{gg} = T_{g(\text{linear, infinite})} + K_x\rho \qquad (15)$$

The cross-link density can be determined by the recursive finite chain probability technique as a function of the extent of reaction. Note that a trifunctional cross-linking unit is considered to be a half tetrafunctional unit since the latter is mechanically equivalent to two of the former. The parameter K_x can be determined by considering the fully cured material in eq 14,

$$K_x = \frac{1}{A_0}(T_{g(\text{fully cured})} - T_{g(\text{linear, infinite})}) \qquad (16)$$

where A_0 is the initial amine concentration.

T_g can be calculated as a function of conversion using eq 11 prior to gel point and eqs 12−16 for conversion after the gel point. Experimentally, a small amount of the mixture was transferred to a DSC pan and the temperature ramped to partially cure. The extent of reaction was determined by the heat flow. Figure 6 represents the calculation results of T_g over the entire conversion range compared to the experimental results. The model provides a good correlation for the experimental data over the entire conversion range, although a few of the data at high conversion appear to lie below the calculated results. One reason for this discrepancy may be due to the DSC technique tending to underestimate the residual exotherm in the high conversion range, and, consequently, the conversion results estimated from the experimental exotherm can be higher than the actual conversion.

Chemorheology. (a) Chemorheology of Epoxy Resin. Cross-linking polymerizations undergo a pseudophase transition from liquid to solid at a critical extent of reaction. The gel point of a chemically cross-linking system is clearly defined as the instant at which the weight-average molecular weight diverges. Chemically cross-linking systems at the gel point have a limiting behavior,[19]

$$\tau(t) = S\int_{-\infty}^{t}(t - t')^{-n}\gamma(t)\,dt' \qquad (17)$$

where $\tau(t)$ is the time-dependent shear stress and $\gamma(t)$ is the time-dependent shear strain. Equation 17 describes the stress in a critical gel that is deformed at a rate $\gamma(t)$, $-\infty < t' < t$. As a consequence, the dynamic mechanical behavior at the gel point is given by dynamic moduli,

$$G'(\omega) \sim G''(\omega) \sim \omega^n \qquad (18)$$

and a loss tangent,

$$\tan\delta = G''(\omega)/G'(\omega) = \tan(n\pi/2) \qquad (19)$$

tan δ is independent of frequency at the gel point with G' and G'' having the same power-law frequency dependence. In this work, eq 19 is applied to determine the gel point from the congruency of tan δ with frequency.

The dynamic moduli and loss tangent of the neat epoxy system during reaction are shown in Figure 7;

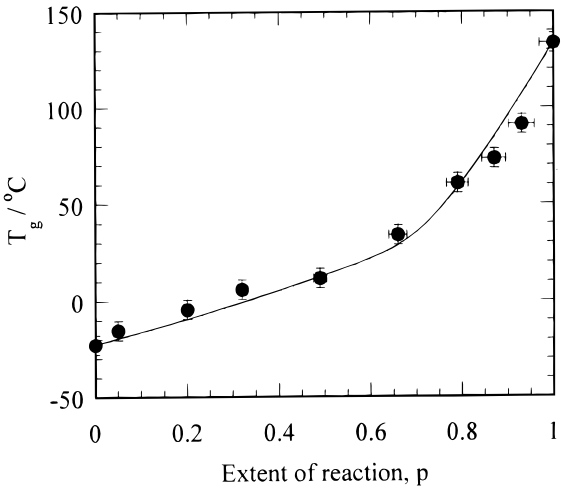

Figure 6. Glass transition temperature of the epoxy/DETDA system as a function of extent of reaction, *p*. The solid line is a calculated result from Gillham's treatment.[14]

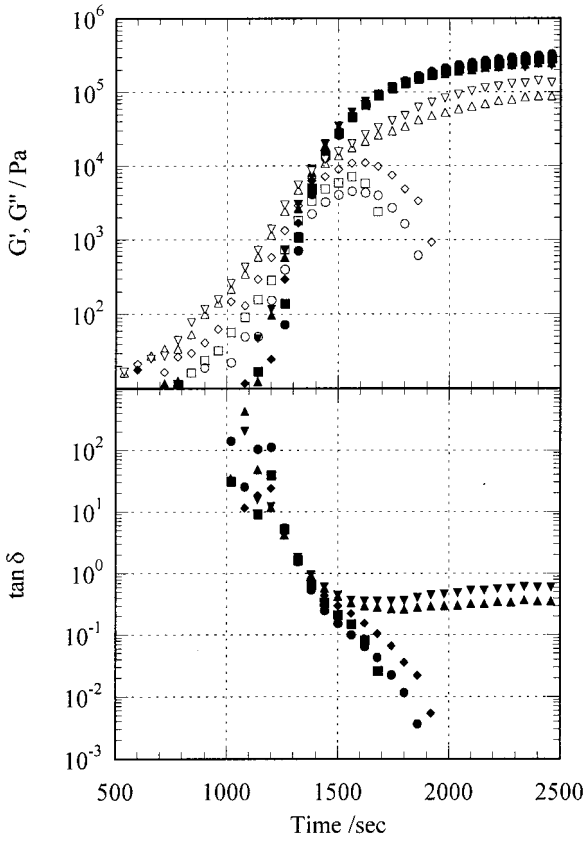

Figure 7. Evolution of the storage modulus (closed symbols), loss modulus (open symbols), and tan δ (closed symbols) during cross-linking of epoxy with DETDA isothermally cured at 150 °C. Applied frequencies are 10 (●, ○), 20 (■, □), 40 (◆, ◇), 80 (▲, △), and 100 Hz (▼, ▽).

an increase in the storage modulus G' of several orders of magnitude occurred during isothermal curing. Subsequently, the G'' curve crosses the G', and finally there is a slow increase in the storage modulus that levels off in the final stage of the reaction. Figure 7 clearly shows a coincidence domain of the time evolution of the tan δ curves obtained at different frequencies. The dynamic mechanical behavior of the gelling epoxy solution can be evaluated as a function of reaction time. The resulting modulus curves near the gel point are shown in Figure 8a,b. At short curing times, the limiting behavior

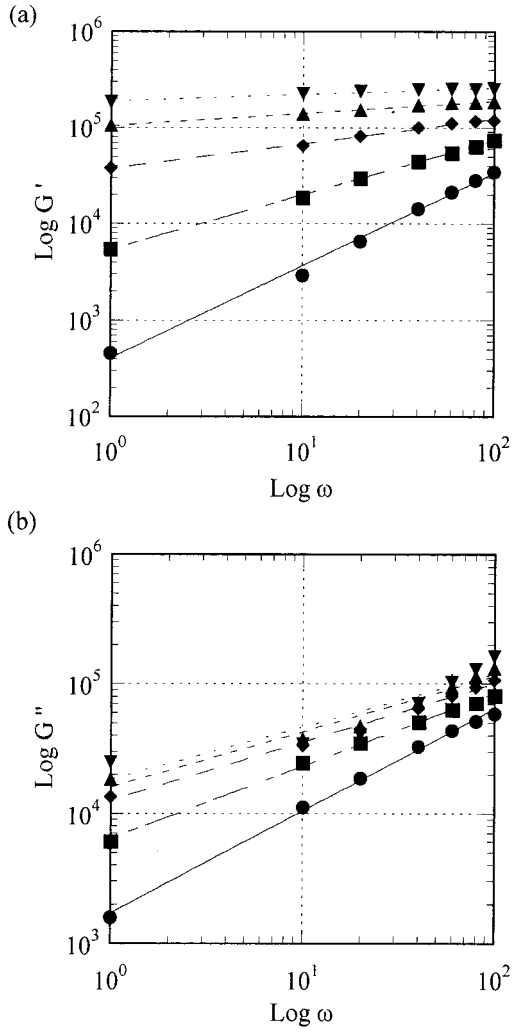

Figure 8. Storage modulus (a) and loss modulus (b) of epoxy/DETDA plotted against curing time for several frequencies near gel point. The curing temperature is 150 °C. Curing time is (●) 1200, (■) 1260, (◆) 1320, (▲) 1380, and (▼) 1440 s.

in the liquid state is observed as[20]

$$G'(\omega) \sim \omega^2 \text{ and } G''(\omega) \sim \omega \quad (\text{at } \omega \to 0) \qquad (20)$$

while the solid state after sufficiently long curing results in a storage modulus,

$$G'(\omega) = \text{constant} \quad (\text{at } \omega \to 0) \qquad (21)$$

The limiting behavior of the dynamic storage modulus indicates that the system behaves like a Newtonian liquid before the gel point and tends to the behavior of a classical network after the gel point.

The slope of the modulus is theoretically predicted by the Rouse model and the Zimm model.[21] The Zimm model examines a high molecular weight polymer in a good solvent. The frequency response of this system is dominated by hydrodynamic interactions between sections of the same macromolecule. In contrast, the Rouse model applies to a system where the concentration of the high molecular weight polymer is increased such that hydrodynamic interactions are completely screened out by polymer coil overlap. At the gel point the viscoelastic behavior extends throughout the frequency range, and the slope of the modulus is frequency-independent. For the Zimm model (hydrodynamic interaction) the prediction of the frequency-independent, congruent gradient is $^2/_3$. Chemical bond percolation predicts $n = {}^2/_3$, as hydrodynamic interactions are assumed in the theoretical derivation. The frequency-independent congruent gradient for the Rouse model (hydrodynamic interaction screened) is $n = {}^1/_2$. Thus, the value of the viscoelastic scaling exponent n is nonuniversal and varies in the range $0.50 < n < 0.67$, when hydrodynamic screening only is considered.[22]

In this system, transition from liquid to solid is fast, and it is difficult to determine the exact viscoelastic nature at the gel point. However, the frequency-independent congruent gradient for this system can be estimated from frequency sweeps of G' and G'', and the congruency of n for G' and G'' is located at $n = 0.66$, which is that predicted by the Zimm model.

The gel times of epoxy/DETDA for several isothermal conditions are summarized in Table 2. From the kinetic study described in previous section, the conversion at the gel point can be determined. The conversions were independent of curing conditions and agree with the theoretical conversion (0.58). The gel times listed in the table are then treated with an Arrhenius relationship (eq 22) and are shown in Figure 9.

$$t_{gel} = Ae^{-E_a/RT} \qquad (22)$$

where E_a is the activation energy, T is the absolute

Table 2. Summary of the Gel Time and Corresponding Conversion of Epoxy and the PPE/Epoxy Blends

sample	T_{cure}/°C	t_{gel}/s	n	p_{gel}	E_a/kJ mol^{-1}
PPE/epoxy	150	960 ± 30	0.60	0.31 ± 0.01	61.9
(PPE 30 wt %)	160	692 ± 30	0.63	0.34 ± 0.01	61.9
	175	376 ± 15	0.62	0.47 ± 0.03	61.9
PPE/epoxy	150	1005 ± 30	0.66	0.27 ± 0.01	63.8
(PPE 40 wt %)	160	690 ± 30	0.61	0.31 ± 0.01	63.8
	175	392 ± 15	0.62	0.41 ± 0.03	63.8
PPE/epoxy	150	1100 ± 30	0.69	0.26 ± 0.01	59.1
(PPE 50 wt %)	160	675 ± 30	0.65	0.26 ± 0.01	59.1
	175	382 ± 15	0.66	0.38 ± 0.01	59.1
	150	1304 ± 30	0.63	0.58 ± 0.01	66.9
epoxy	160	850 ± 30	0.64	0.60 ± 0.01	66.9
	175	468 ± 30	0.65	0.60 ± 0.03	66.9

[a] T_{cure} = curing temperature, t_{gel} = gel time, n = gelation exponent, p_{gel} = gel conversion, E_a = activation energy.

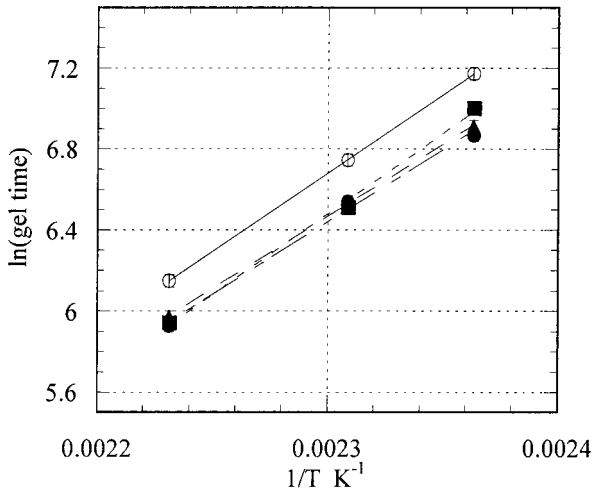

Figure 9. Arrhenius plot of the gel time for epoxy (○) and PPE/epoxy system. PPE content is (●) 30 wt %, (▲) 40 wt %, and (■) 50 wt %.

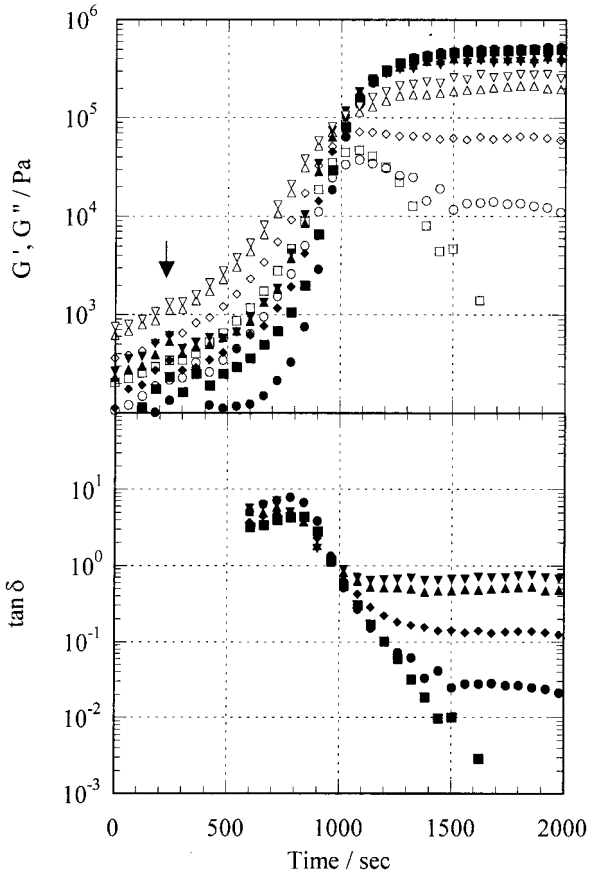

Figure 10. Evolution of the storage modulus (closed symbols), loss modulus (open symbols), and tan δ (closed symbols) during cross-linking of PPE/epoxy/DETDA isothermally cured at 150 °C. Applied frequencies are 10 (●, ○), 20 (■, □), 40 (◆, ◇), 80 (▲, △), and 100 Hz (▼, ▽). The arrow indicates the onset of phase separation.

temperature of reaction, and R is the universal gas constant. The activation of the reaction was calculated to be 66.9 kJ/mol, which is a reasonable value compared to bisphenol A type epoxy resin and aromatic amine compounds.[9]

(b) Chemorheology of PPE/Epoxy Blend. The chemorheological data obtained upon isothermal curing of the PPE/epoxy/amine are shown in Figure 10. The initial value of the modulus is rather high compared to that of the epoxy/DETDA system described previously. The addition of PPE into the epoxy results in a high viscosity of the system. Interestingly, the dynamic storage and loss moduli reflect the characteristics of phase separation during curing. After an induction period, a sudden discontinuous change in moduli (arrowed in Figure 10) was observed. This can be related to the onset of phase separation accompanied by a gradual increase in both moduli due to the structure development of the continuous PPE-rich phase. The storage modulus and loss modulus intersect near the gel point; however, the moduli have nearly reached a maximum value at this point. Figure 10 also shows the time evolution of the tan δ curves obtained at different frequencies. These curves intersect at a single point; i.e., the crossover of the curves marks the gel point. These data are similar to those from the epoxy/DETDA system as previously described and indicate that the material undergoes a transition from the liquid to the solid state. Shortly before the gel point, the material is still a liquid, and the moduli decrease to zero at low frequency.

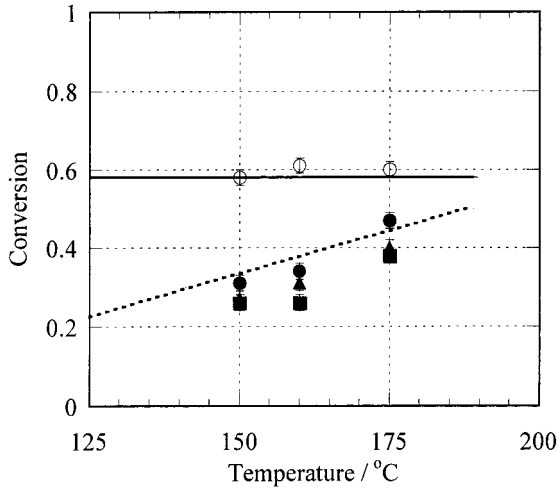

Figure 11. Comparison of the conversion at the gel point of the epoxy (○) and PPE/epoxy system. PPE content is (●) 30 wt %, (▲) 40 wt %, and (■) 50 wt %. The solid line is Flory–Stockmayer's theoretical gel point for the 2-functional epoxy and 4-functional amine system. The dotted line is a simulated result from development of Berghmans' point (see Figures 12 and 14).

Shortly after the gel point, the storage modulus G' tends toward a limiting value at low frequency, demonstrating the permanent elastic characteristics of a solid material. The shapes of both $G'(\omega)$ and $G''(\omega)$ change smoothly as the reaction proceeds and cross over in a continuous fashion. It is difficult to determine the exact viscoelastic nature at the gel point.

The gel points of PPE/epoxy/DETDA for several isothermal conditions are summarized in Table 2 and plotted in Figure 11 as a comparison with the conversion for the neat epoxy system. Figure 9 indicates the Arrhenius plot for the gel time of the blends. Interestingly, the conversion at the gel point is smaller than the neat epoxy system and has a dependency on the curing temperature as shown in Figure 11. While the gelation of the PPE/epoxy mixture is rather different from epoxy itself, the activation energies from the gel point are around 60 kJ/mol and are in quite good agreement with that of the neat epoxy system, i.e., driven by polymerization.

Gelation Mechanism of PPE/Epoxy Blend. The coincidence of the activation energies for the epoxy system and the PPE/epoxy system indicates that the driving force of the gelation is the chemical reaction of epoxy cross-linking. However, this deviation from Flory–Stockmayer's theory has to be explained by an appropriate mechanism.

The mechanism proposed to explain the gelation of the PPE/epoxy system is that gelation occurs by vitrification, i.e., the physical gelation of the PPE-rich phase. A schematic explanation of such a mechanism is shown in Figure 12 as a series of snapshots of phase diagrams during polymerization. Initially, the conversion of epoxy resin is 0%, and the cloud point curve and T_g–composition curve are both set at initial values as shown in Figure 12a. The Berghmans point is the intersection between the cloud point curve and the T_g–composition curve and is initially set at temperature $T = T_0$ and weight fraction of PPE $\phi = \phi_c$. The mixture is vitrified at $T = T_0$ if the composition is below ϕ_c.

When the sample is isothermally polymerized at the temperature $T = T_1$, the reaction of epoxy resin starts, and both cloud point curve and T_g–composition curve

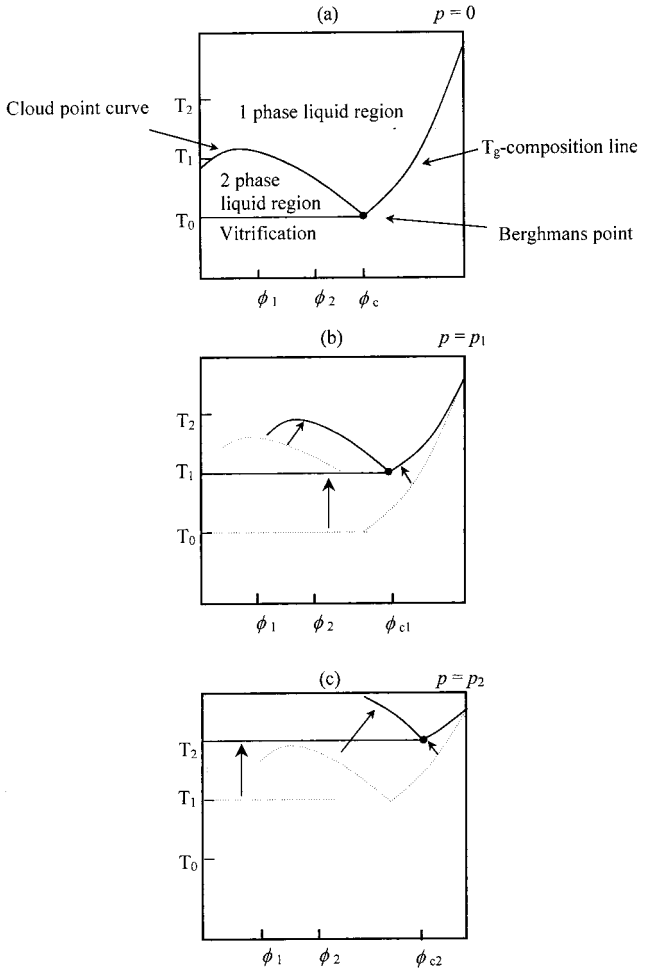

Figure 12. Proposed mechanism for the gelation of the PPE/epoxy blend. (a) Phase diagram at the initial stage. Berghmans' point exists at $T = T_0$ and $\phi = \phi_c$. (b) Phase diagram when the conversion reaches $p = p_1$. Berghmans' point is at $T = T_1$ and $\phi = \phi_{c1}$. (c) Phase diagram when the conversion reaches $p = p_2$. Berghmans' point is at $T = T_2$ and $\phi = \phi_{c2}$.

shift upward due to the increase of molecular weight and T_g of epoxy resin (Figure 12b). Consequently, Berghmans' point is shifted upward. As soon as Berghmans point reaches a temperature $T = T_1$, the PPE-rich phase vitrifies. The vitrification occurs at the same conversion at $p = p_1$, as far as the composition is below Berghmans' point (ϕ_1, $\phi_2 < \phi_{c1}$). If the processing temperature is T_2 ($T_2 > T_1$) as shown in Figure 12c, the vitrification of the PPE-rich phase should occur at a different conversion, p_2 ($>p_1$). This is the reason the gelation of the PPE/epoxy blend depends on the processing temperature.

From the scattering, morphological, and rheological studies, the structure development of the PPE/epoxy blend during polymerization can be illustrated as shown in Figure 13. Initially, the mixture is homogeneous (a). Once the reaction proceeds, the mixture moves into the two-phase region, and demixing takes place via spinodal decomposition (b). This yields a bicontinuous morphology with a characteristic periodicity. After that, bicontinuity is lost, and a spherical domain structure is attained. The continuous PPE-rich phase and epoxy-rich droplets are formed for compositions above the critical point (c). The emergence of the continuous PPE-rich phase results in the discontinuity in the viscoelastic functions during isothermal curing. The cloud point

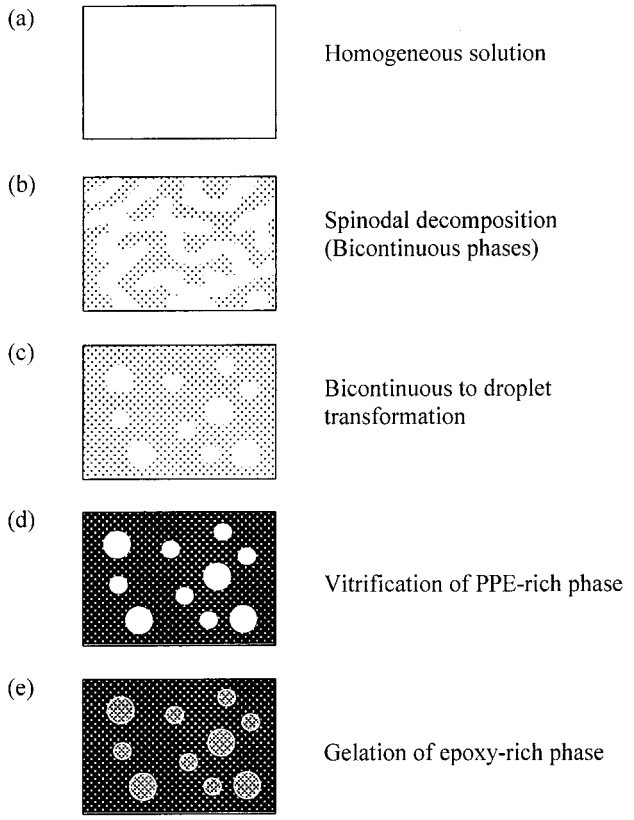

Figure 13. Schematic representation of the structure development during isothermally curing for the PPE/epoxy blends.

curve shifts upward, and the composition of the phases change along with the phase diagram. The PPE-rich phase then reaches Berghmans' point and vitrifies (d). Finally, the conversion reaches the "chemical" gel point, and the reaction is completed (e). This processing method relies on the reaction taking place below the T_g of the PPE. The initial mixture has a $T_g < T$ whereas the in the phase-separated blend the T_g(PPE) $> T$ and solidification occurs by vitrification.

Prediction of Phase Diagram during Reaction. As described in the previous section, the gelling mechanism of the PPE/epoxy mixture during reaction is "physical" gelation (vitrification) of the continuous PPE-rich phase. Since Berghmans' point is the intersection of the T_g−composition curve and the cloud point curve, it is possible to obtain Berghmans' point as a series of "snapshots" of the phase diagram during reaction. Both curves are related to the molecular weight of the epoxy resin. In this section, the phase diagram and the T_g−composition curve are related to the conversion of the epoxy resin. A series of Berghmans' points during the reaction are predicted and compared to the experimental data. The major assumptions are the following: (1) The cloud point can be expressed by the Flory−Huggins theory. (2) The T_g of homogeneous mixtures of PPE and epoxy resin obey the Fox equation. (3) The molecular weight of epoxy resin during processing is calculated using recursive techniques.[17] (4) Interactions between components remain the same throughout the cross-linking process; i.e., Flory's interaction parameter does not appreciably change during polymerization of epoxy resin for isothermal processing. (5) The initial degree of polymerization of epoxy resin is 2. That of PPE is 242.

Table 3 summarizes the information used in this simulation. Several values of conversions (10%, 20%,

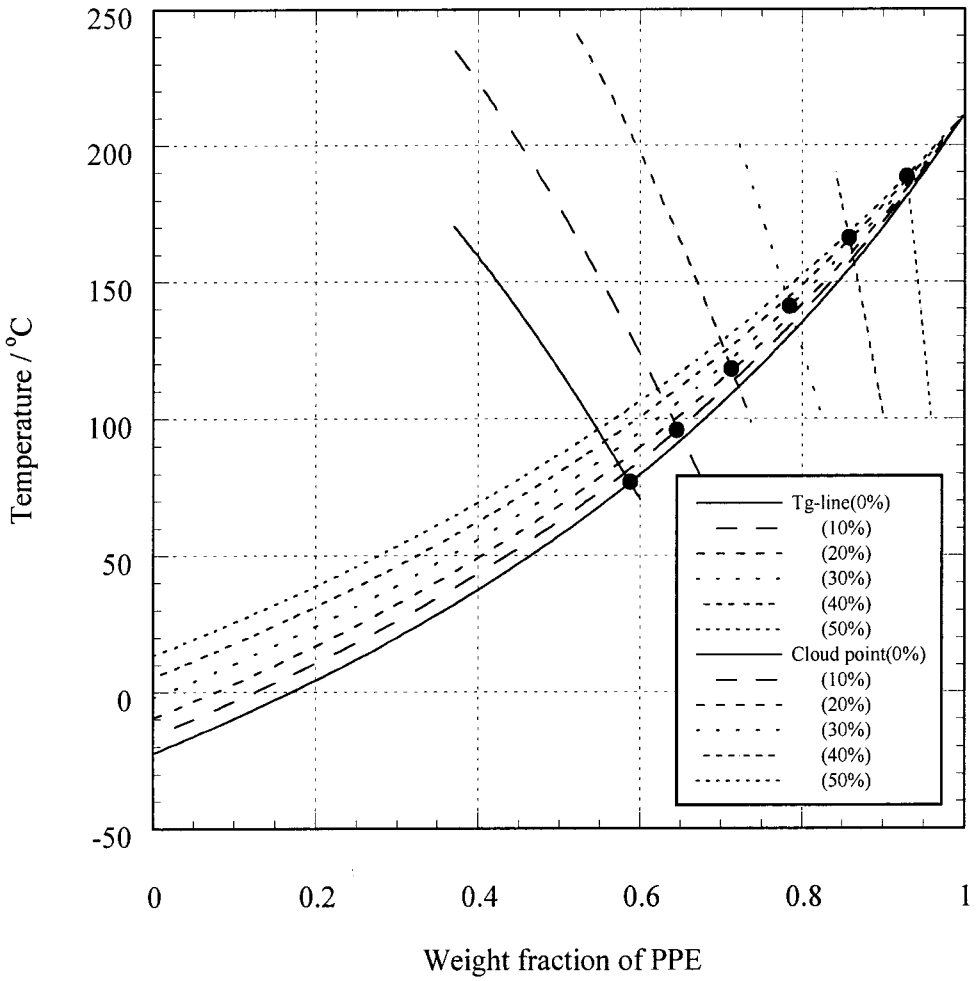

Figure 14. Predicted phase diagram evolution during curing for a PPE/epoxy/DETDA system. Berghmans' points are shown as dots.

Table 3. Physical Constants and Parameters Used in the Calculation of the Phase Diagram and the T_g−Composition Line for the PPE/Epoxy System

items	values
Epoxy Resin	
degree of polymerization (M_n), for conversion =	
0	2.00 (313.6)
0.1	2.31 (361.8)
0.2	2.73 (427.6)
0.3	3.33 (522.6)
0.4	4.29 (671.9)
0.5	6.00 (940.7)
T_g/°C, for conversion =	
0	−22.6
0.1	−16.2
0.2	−9.3
0.3	−2.4
0.4	5.3
0.5	13.3
PPE	
degree of polymerization (M_n)	242 (29000)
T_g/°C	211
Flory−Huggins χ parameter	$\chi = 145/T + 0.002$
gas constant	8.3145 J K^{-1} mol^{-1}

30%, 40%, and 50%) were selected for this calculation. The Flory−Huggins interaction parameter was used assuming its temperature dependence given by $\chi = a + b/T$. Figure 14 illustrates the T_g−composition curves and cloud point curves for conversion of epoxy resin 0 to 0.5.Intersections corresponding to each conversion are also plotted on the phase diagram. The cloud point curves shift toward higher temperature with the conversion of epoxy resin. The T_g−composition curve shows, however, a small shift toward higher temperature. It is obvious that the influence of the cloud point curve for PPE/epoxy resin is dominant on the position of Berghmans' point during the reaction. The dotted line in Figure 11 shows a comparison of the simulation to the experimental data. The predicted gelation point shows a good agreement with the experimental data as the gel point shift linearly toward higher temperature during isothermal curing. Calculated results show unambiguously that the gelation of PPE/epoxy resin is the "vitrification" of the continuous PPE-rich phase. This prediction can be applied to estimation of the gel point of other thermoplastic/thermoset blends. The gel point is the transition from Newtonian to non-Newtonian fluid behavior for both physical and chemical gelation. Thus, predicting the gel point for thermoplastic/thermoset blends is a useful tool for designing polymer processing operation, especially for printed circuit boards where there is a need to fill very narrow lines and spaces without any voids.

Conclusions

The chemorheological study of a series of PPE/epoxy blends was investigated using rheology and DSC. Gelation was followed by dynamic mechanical measurement, and the gel point was determined as a congruency

in the time evolution of the tan δ curves obtained at different frequencies. The gel point of epoxy/DETDA was at a conversion of epoxy ~0.60, which agreed with the theoretical conversion (0.58) from Flory−Stockmayer's gelation theory.[8] The gel point of PPE/epoxy/DETDA was also investigated, and the gel point was found at conversions between 0.20 and 0.40, below the chemical gel point of the epoxy, indicating that the gelation mechanism was physical rather than chemical. The coincidence of the activation energies for the epoxy system and the PPE/epoxy system indicates that the driving force of the gelation is the chemical reaction of epoxy polymerization which moves phase boundaries and causes phase separation. The mechanism proposed to explain the gelation of the PPE/epoxy system is that gelation occurs by vitrification, i.e., the physical gelation of the PPE-rich phase. The nature of the glass transition of the PPE in the blend caused gelation by phase separation and vitrification of the PPE-rich phase. Using Flory−Huggins theory and Macosko's recursive theory, the shift of Berghmans' point during processing is successfully simulated.

References and Notes

(1) Halley, P. J.; Mackay, M. E. *Polym. Eng. Sci.* **1996**, *36*, 593.
(2) Flory, P. J. *J. Chem. Phys.* **1941**, *9*, 660.
(3) Huggins, M. L. *J. Chem. Phys.* **1941**, *9*, 440.
(4) Goosens, J. G. P.; Rastogi, S.; Meijer, H. E. H.; Lemstra, P. J. *Polymer* **1998**, *39*, 6577.
(5) Kim, B. S.; Chiba, T.; Inoue, T. *Polymer* **1993**, *34*, 2809; **1995**, *36*, 67.
(6) Callister, S.; Keller, A.; Hikmet, R. M. *Makromol. Chem., Makromol. Symp.* **1990**, *39*, 19.
(7) Clarke, N.; McLeish, T. C. B.; Jenkins, S. D. *Macromolecules* **1995**, *28*, 4650.
(8) Elliniadis, S.; Higgins, J. S.; Clarke, N.; McLeish, C. B.; Choudhery, R. A.; Jenkins, S. D. *Polymer* **1997**, *38*, 4855.
(9) (a) Sperling, L. H.; Mishra, V. *Polym. Adv. Technol.* **1996**, *7*, 197. (b) Mishra, V.; Du Prez, F. E.; Gosen, E.; Goethals, E. J.; Sperling, L. H. *J. Appl. Polym. Sci.* **1995**, *58*, 331.
(10) Ishii, Y.; Ryan, A. J. *Macromolecules* **2000**, *33*, 158.
(11) Rozenberg, B. A. *Adv. Polym. Sci.* **1986**, *75*, 113.
(12) Horie, K.; Himura, H.; Sawada, I.; Mita, I.; Kambe, H. *J. Polym. Sci., A-1* **1970**, *8*, 1357.
(13) Kamal, M. R. *Polym. Eng. Sci.* **1974**, *14*, 231.
(14) Wisanrakkit, G.; Gillham, J. K. *J. Appl. Polym. Sci.* **1990**, *41*, 2885.
(15) Yang, W. P.; Macosko, C. W. *Die Makromol. Chem. Macromol. Symp.* **1989**, *25*, 23.
(16) Hale, A.; Mackosko, C. W.; Bair, H. E. *Macromolecules* **1991**, *24*, 2610.
(17) Macosko, C. W.; Miller, D. R. *Macromolecules* **1976**, *9*, 199.
(18) Fox, T. G.; Loshaek, S. *J. Polym. Sci.* **1995**, *15*, 371.
(19) Chambon, F.; Winter, H. H. *Polym. Bull.* **1985**, *13*, 499. Chambon, F.; Winter, H. H. *J. Rheol.* **1987**, *31*, 683.
(20) Chambon, F.; Petrovin, Z.; MacKnight, W. J.; Winter, H. H. *Macromolecules* **1986**, *19*, 2146.
(21) Ferry, J. D. *Viscoelastic Behavior of Polymers*; Wiley & Sons: New York, 1980.
(22) Griffith, I. W. Ph.D Thesis, UMIST, 1996.

MA990838A